Synthesis and Consolidation of Powders Based on Si_3N_4–Zr

I. Kud, L. I. Ieremenko, L. A. Krushynska, D. P. Zyatkevych, O. B. Zgalat-Lozynskyi, and O. V. Shyrokov

1 Introduction

The complex of the physicomechanical and chemical properties of porousless nanocomposites with a ceramic matrix based on Si_3N_4 and reinforced by nanosized particles of carbides and nitrides of transition metals makes them promising candidates for the development of next-generation ceramic bearings and seals intended for operation under conditions of severe friction. For instance, the introduction of zirconium nitride into the silicon nitride matrix makes it possible to enhance the corrosion resistance due to the formation of insoluble oxide layers, which provides the self-healing effect of the material. During contact in an aqueous medium, a gel that has a larger volume and protects grains boundaries against subsequent corrosion forms [1].

The low chemical activity of these ceramic materials, high oxidation resistance, and extremely low porosity of products manufactured from them by the spark plasma sintering (SPS) method guarantee increased operating characteristics of rolling and plain bearings intended for operation under severe conditions in corrosive-erosive media without lubrication.

In the development of new silicon nitride composite powder materials with a uniform distribution of components and a homogeneous character of development of structural transformation, it is reasonable to use precursors containing all elements required for the synthesis of the final composition. In this case, the main requirements for precursors are as follows:

I. Kud (✉) · L. I. Ieremenko · L. A. Krushynska · D. P. Zyatkevych · O. B. Zgalat-Lozynskyi · O. V. Shyrokov
Frantsevych Institute for Problems of Materials Science of NAS of Ukraine, Krzhyzhanovsky St., 3, Kiev 03142, Ukraine
e-mail: eli123@ukr.net

– the thermodynamic instability at relatively low temperatures as compared with the thermodynamic stability of interaction products;
– the completeness of the reaction.

Our previous investigations in the development of methods for preparing nanopowders of nitride composite materials [2] and the literature data [3, 4] indicate the prospects of using silicides of transition metals containing all components of their nitriding products as initial components (precursors). However, the use of disilicides as precursors restricts the possibility of preparing nitride composite materials in a wide concentration range [3].

The aim of the present work is to investigate the synthesis of nanodisperse composite powders of the Si_3N_4–ZrN system in a wide concentration range and their consolidation.

2 Experimental Technique

During phase transformations in the process of decomposition of complex substances, high-activity ingredients, which are initial components in the synthesis of new compounds, form [4]. The interaction of a transition metal with silicon nitride in vacuum is an example of such a process. The metal accelerates the dissociation process of silicon nitride at temperatures much lower than the decomposition temperature of pure Si_3N_4 in vacuum. Due to the decomposition of Si_3N_4 into high-activity silicon and nitrogen, in the process of their interaction with the metal in vacuum, the possibility of obtaining a disperse product, namely, metal nitride or silicide, arises [5].

Zirconium and β-Si_3N_4 powders were used as initial materials. The commercial zirconium powder (PTsE grade) had a mean particle size of 20 μm. The β-Si_3N_4 powder synthesized under laboratory conditions had a specific surface of 3.8 m^2/g and nitrogen content of 38.0 mass%. Reaction mixtures were calculated according to the following reaction:

$$Si_3N_4 + 4Zr = 4ZrN + 3Si. \tag{1}$$
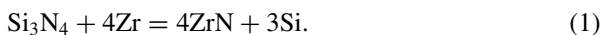
To provide a uniform distribution of elements, the components were mixed in a Pulverizette–6 planetary mill (FRITSCH GmbH, Germany) in ethanol in a drum with silicon nitride grinding balls. During mixing, the particle size did not change. Homogenized reaction mixtures were heat-treated in an SNV–1.3,1/20–I1 electric vacuum furnace in a vacuum of ~1 × 10^{-3} Pa in the temperature range 750–1450 °C and in a nitrogen atmosphere at temperatures of 1000–1200 °C.

The products of the solid-state interaction in a vacuum and a nitrogen atmosphere were investigated by the XRD method on a DRON-3 diffractometer in filtered Cu-$K\alpha$ radiation. The nitrogen and zirconium contents in the final product were determined

by the chemical analysis method according to standard techniques (GOST 27417-87). The evaluation of the particle size of the synthesized powder was performed in a CILAS 990 laser particle size analyzer. Microstructural studies were carried out with a Superprobe-733 scanning electron microscope.

The consolidation of the obtained Si_3N_4–ZrN composite powders was performed by the spark plasma sintering method using an HD25 unit (FCT Systeme GmbH, Germany) (maximal temperature of 2400 °C, maximal pressing pressure of 250 kN, maximal current of 8000 A, maximal voltage of 10 V, media are a vacuum of 5×10^{-2} mbar and nitrogen). Powder mixtures in amounts of about 8 g were loaded into a graphite die with two graphite punches. The temperature on the internal surface of the upper graphite punch was measured with a digital pyrometer.

3   Results and Discussion

The investigation of the behavior of the β-Si_3N_4 + 4Zr reaction mixture in a vacuum under the action of the temperature factor (Table 1) showed that already at a temperature of 750 °C, solid-state interaction occurs. Along with the β-Si_3N_4 phase, in the products of heat treatment at a temperature of 750 °C, the α-$ZrN_{0.28}$ solid solution and ZrN phase, formed by the mechanism of contact diffusion, were recorded. This is connected with the self-diffusion rate of nitrogen in β-Si_3N_4 ($D_i = 6.8 \times 10^2 \exp(-777.5/RT)$ m^2/s). The solubility of nitrogen at this temperature in α-Zr is equal to 4.8 mass% [6].

An increase in the treatment temperature up to 1000 °C leads to the formation of nitride (α-Zr_2N and ZrN) and silicide (Zr_5Si_3, Zr_2Si, and ZrSi) phases of zirconium. Moreover, free silicon and the α-Si_3N_4 phase are present. The product of solid-state interaction at a temperature of 1450 °C is a mixture of ZrN, $ZrSi_2$, and a small amount of β-Si_3N_4. At a temperature of 1450 °C, the complete dissociation of silicon nitride occurs, and the main phases are ZrN and lower zirconium silicides. According to the chemical analysis data, the nitrogen content in the interaction products remains practically unchanged and is nearly equal to its calculated content in the (Si_3N_4 + 4Zr) initial reaction mixture (9.8 mass%). This indicates that practically the whole amount of nitrogen took part in the solid-state interaction.

Table 1 Results of solid-state interaction in vacuum for 1 h

Reaction mixture (mass%)	Temperature (°C)	Phase composition	Nitrogen content (mass%)
28β-Si_3N_4 + 78Zr	750	β-Si_3N_4, α-$ZrN_{0.28}$, ZrN	9.9
	1000	β-Si_3N_4, ZrN, α-Zr_2N, Zr_5Si_3, Zr_2Si, ZrSi, Si, α-$Si_3N_{4(traces)}$	9.6
	1450	ZrN, $ZrSi_2$, β-Si_3N_4	9.3

Thus, as a result of the dissociation of Si_3N_4, the solid-state interaction in vacuum occurs by the mechanism of reaction diffusion on interfaces of zirconium and silicon nitride particles. This suggests that the formation of the composite material occurs on particles of initial zirconium. The diffusion of nitrogen into zirconium at 750 °C is accompanied by the formation of zirconium nitrides, and the diffusion of silicon at 1000 °C is accompanied by the formation of the lower silicide phases Zr_2Si, $ZrSi$, and Zr_5Si_3. This testifies the reasonability of using the high-activity product of vacuum solid-state interaction at 1000 °C as a precursor for subsequent nitriding. The realization of these operations in a single technological process is economically sound.

The process of subsequent nitriding in a single cycle of the product of preliminary vacuum heat treatment of the β-Si_3N_4 + 4Zr mixture was investigated in the temperature range 1000–1200 °C for 1 h. Characteristics of the final product according to the XRD and chemical analysis data are presented in Table 2.

The analysis of the presented data indicates that, at a nitriding temperature of 1200 °C, the phase composition of the product is ZrN and β-Si_3N_4.

Thus, the optimal synthesis regime of the Si_3N_4–ZrN composite material in a single cycle is vacuum treatment at 1000 °C (stage 1) and nitriding at 1200 °C for 1 h (stage 2). The final product contains only nitride phases of zirconium and silicon. The nitrogen content in the product is equal to its content calculated by reaction (1).

The possibility of obtaining a Si_3N_4–ZrN composite material in a wide concentration range in the established optimal synthesis regime was investigated.

In Fig. 1, X-ray diffraction patterns of the products of the two-stage synthesis of reaction mixtures of different composition are shown. The XRD data analysis indicates that, for all investigated compositions, a two-phase product, in which the ZrN content ranged from 11 up to 33 vol.%, was obtained. It should be noted that in the X-ray diffraction patterns of the mixtures with a ZrN content of 11 and 22 vol.%, traces of $ZrSi_2$ are also present.

The chemical analysis data of the synthesis products (Table 3) in the established regime show that the combination of heat treatment at 1000 °C in vacuum with subsequent nitriding at 1200 °C in a single technological process makes it possible to obtain powders of the composite materials, the nitrogen contents in which are maximally close to the theoretical ones.

Table 2 Characteristics of the product of the two-stage heat treatment of the 22 mass% β-Si_3N_4 + 78 mass% Zr mixture for 1 h

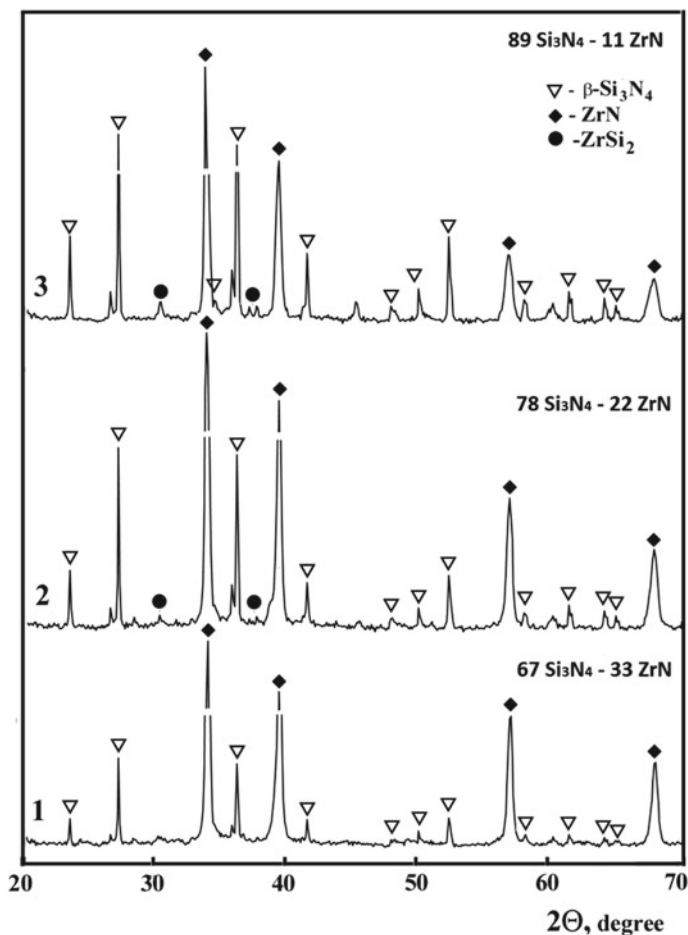| Synthesis regime		Phase composition	Nitrogen content (mass%)
Stage 1 (vacuum)	Stage 2 (nitrogen)		
Temperature (°C)	Temperature (°C)		
1000	1000	ZrN, β-Si_3N_4, $ZrSi_2$	11.7
1000	1100	ZrN, β-Si_3N_4, $ZrSi_2$	12.7
1000	1200	ZrN, β-Si_3N_4	13.1

Fig. 1 X-ray diffraction patterns of the products of the two-stage synthesis from reaction mixtures of different composition: (**1**) 67 vol.% Si$_3$N$_4$–33 vol.% ZrN, (**2**) 78 vol.% Si$_3$N$_4$–22 vol.% ZrN, (**3**) 89 vol.% Si$_3$N$_4$–11 vol.% ZrN

Table 3 Certification of composite materials

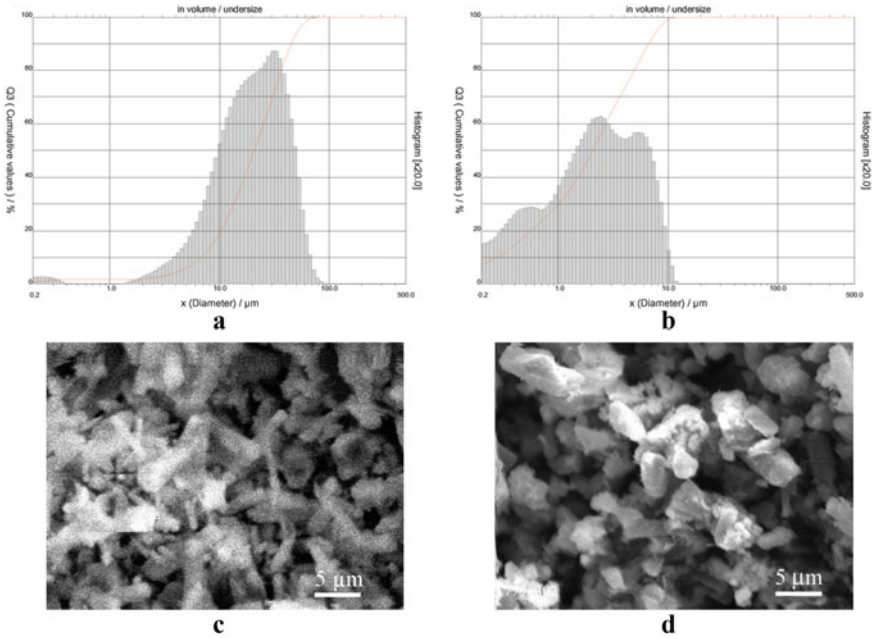| Composition of the reaction mixture (mass%)	Chemical analysis data (mass%)				Specific surface (m²/g)	Final composition of the synthesized product (vol.%)	Resistivity (μΩ̂ cm)
	N		Zr	Fe			
	Theor.	Exp.					
50Si$_3$N$_4$–50Zr	23.8	20.8	48.7	1.9	3.46	67Si$_3$N$_4$ + 33ZrN	104 × 10^5
64Si$_3$N$_4$–36Zr	25.4	26.5	31.8	1.2	5.14	78Si$_3$N$_4$ + 22ZrN	147 × 10^5
80Si$_3$N$_4$–20Zr	29.7	28.9	22.8	0.5	5.87	89Si$_3$N$_4$ + 11ZrN	309 × 10^{16}

Fig. 2 Particle-size distribution of the 78 vol.% Si_3N_4–22 vol.% ZrN composite powder after synthesis (**a**) and dispersion (**b**) and the morphology of the initial mixture (**c**) and synthesized powder (**d**)

According to the data of evaluation of the particle size of the synthesized 78 vol.% Si_3N_4–22 vol.% ZrN composite powder, the mean size of agglomerates is 23.71 µm (Fig. 2a). After dispersion in isopropyl alcohol, the mean particle size decreased by an order of magnitude down to 2.81 µm (Fig. 2b), and, moreover, the number of submicron and nanosized particles increased.

The analysis of the morphology testifies (Fig. 2d) that the obtained product consists of agglomerates of the Si_3N_4–ZrN composite powder. A comparison of the morphology of the initial mixture based on β-Si_3N_4 (Fig. 2c) with the morphology of the synthesized powder indicates that the shape of particles radically changes from the elongated to the rounded one.

Thus, it is established that the process of vacuum treatment of the Si_3N_4 + Zr reaction mixtures at a temperature of 1000 °C makes it possible to obtain precursors containing the necessary initial components of the nitride ceramics. The combination of the vacuum heat treatment and nitriding (at 1200 °C) processes in a single cycle leads to obtaining disperse powders of the Si_3N_4–ZrN composite materials in a wide concentration range (11–33 vol.% ZrN).

Zirconium nitride, which exhibits high electrical conductivity, strength, and melting point, meets the main requirements to the conductive hardening phase in silicon nitride [1]. Since the difference between the electrical resistivity of silicon nitride (~10^{13}–10^{14} µΏ × cm) and electrical resistivity of zirconium nitride (29 µΏ ×

cm) is extremely large, the electrical conductivity of the composite ceramics depends primarily on the continuity of the conductive 3D network of ZrN particles, the content of ZrN, and the homogeneity of its distribution in the composite ceramics [7, 8].

The conductivity of composite ceramics of the Si_3N_4–ZrN system, as ceramics of a typical insulator–conductor system, must show the percolation behavior, which is characterized by an abrupt decrease in the electrical resistivity at a certain content of the conductive phase [9]. The content of the conductive phase at which a conductive network form is called the percolation concentration or percolation threshold. Since this parameter depends to a great extent on technological regimes of preparation of the material, dispersity, and shape of particles, it is most reasonable to determine it experimentally from concentration dependences of conductivity [7]. For the obtained Si_3N_4–ZrN composite powders, the values of the electrical resistivity were determined (Table 2).

4 Spark Plasma Sintering of Si_3N_4–ZrN Composites

Data on the linear shrinkage of the Si_3N_4–ZrN composite powders in the process of SPS consolidation were monitored as the travel distance of the upper punch (the bottom punch is fixed) and converted into the shrinkage rate of specimens. After loading of about 8 g of the composite powder into the graphite die 20 mm in diameter with a punch unit, a pressure of 50 MPa was applied to establish good contacts between the graphite tools and powder particles. Sintering experiments were performed in the nonlinear consolidation regime developed earlier [10–12]. The Si_3N_4–ZrN composites were consolidated in few-stage regimes, in which pressure was sequentially increased from 50 up to 80 MPa and the heating rate was decreased from 100 °C/min down to 20 °C/min. The temperature was measured by a pyrometer on the inner surface of the upper graphite punch. Isothermal holding for 1.5 min at high temperatures was used to fully densify the Si_3N_4–ZrN composites.

All investigated Si_3N_4–ZrN composites were densified at a temperature of 1750 °C withholding for 5 min. The analysis of the sintering curves shows that the densification process proceeds in two stages (Figs. 3 and 4). The first stage of densification takes place in the temperature range of 400–800 °C. This can be connected with the increase in the pressure, destruction of strong agglomerates in the powder mixture, and rearrangement of particles.

As expected, the composite with 33 vol.% ZrN demonstrates the highest sinterability (Fig. 3, curve 1). This is connected with the large content of the highly conductive phase in the mixture, which forms a branched continuous network of ZrN particles. The densification of the 67 vol.% Si_3N_4–33 vol.% ZrN composite starts at a temperature of 1200 °C and proceeds quite intensively at a shrinkage rate of 1 mm/min up to a temperature of 1600 °C (Fig. 4, curve 1). This agrees well with the character of SPS densification curves of ZrN nanogranular powder (Fig. 5) synthesized by the method of carbothermal reduction-nitriding of a precursor obtained by the sol–gel method (the size of the coherent scattering region is 48 ± 2 nm). The
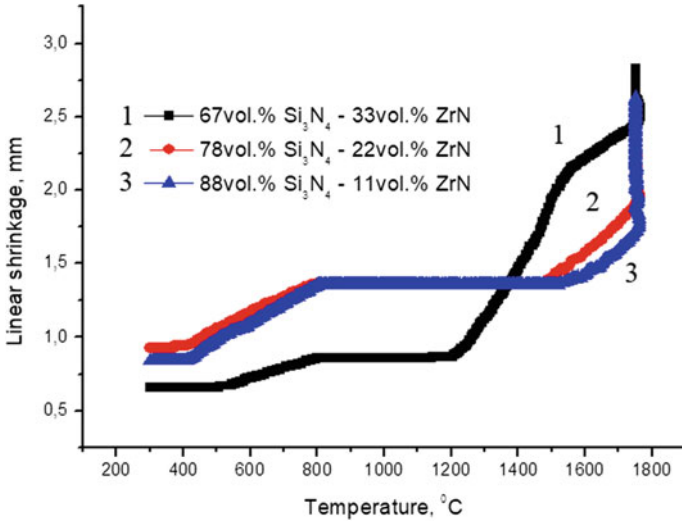
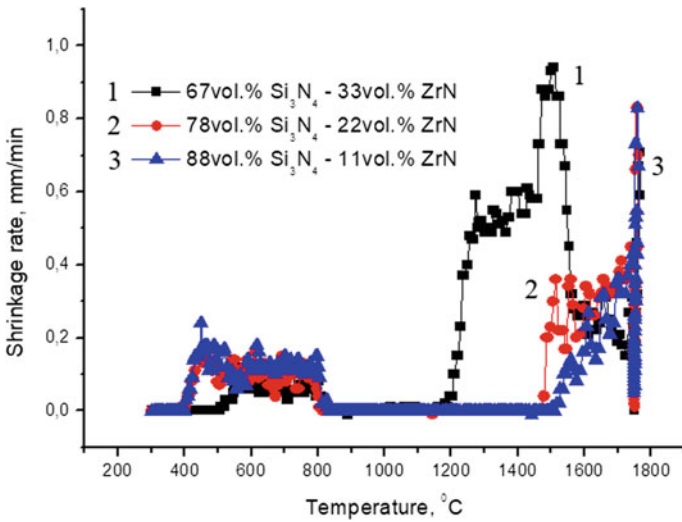**Fig. 3** Linear shrinkage versus temperature for SPS consolidated Si_3N_4–ZrN composites

Fig. 4 Shrinkage rate versus temperature for SPS consolidated Si_3N_4–ZrN composites

comparison of the values of the electrical resistivity of ZrN (29 $\mu\acute{\Omega} \times$ cm) and the composite material with 33 vol.% ZrN (104×10^5 $\mu\acute{\Omega}$ cm) enables us to argue that, in the process of consolidation by the SPS method, due to the formation of the continuous 3D network of ZrN particles, the run of the densification curve of the composite is analogous to that for zirconium nitride. In holding at a temperature of
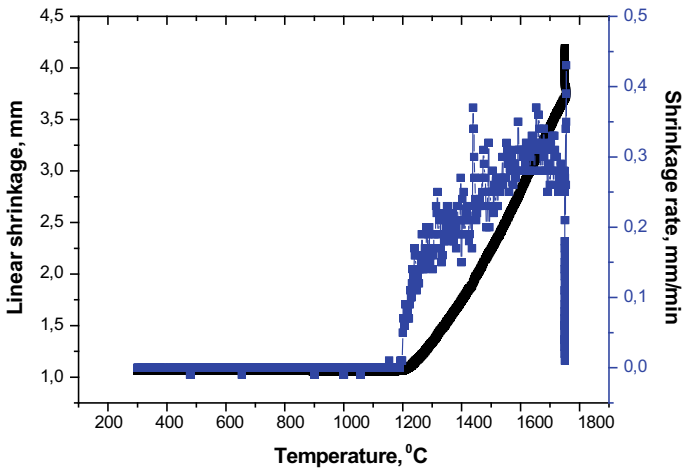
Fig. 5 Linear shrinkage and shrinkage rate versus temperature for SPS consolidated ZrN

1750 °C, minor densification occurs, and the density attains 97% of the theoretical one.

The composites with 22 and 11 vol.% ZrN demonstrate similar conditions of densification during SPS (Fig. 3, curves 2 and 3). For the composites, densification begins at a temperature about 1400 °C and the most intensive phase of shrinkage with a shrinkage rate of 0.9 mm/min is observed during holding at 1750 °C. This can be explained by the low content of the conductive phase (ZrN), which is below the percolation threshold. In contrast to the composite with 33 vol.% ZrN, where densification process is controlled by the ZrN phase, for the composites with 22 and 11 vol.% ZrN, where traces of zirconium disilicide are present (Fig. 1, curves 2 and 3), the sintering process is activated by its phase transformation into zirconium nitride.

The microstructure of the sintered 78 vol.% Si_3N_4–22 vol.% ZrN specimen shown in Fig. 6, indicates the size inhomogeneity of both the ZrN phase (light grains) and Si_3N_4 phase (dark grains). The ZrN phase has the relatively narrow grain size range 200–400 nm, whereas the Si_3N_4 phase, whose fraction is about 80 vol.%, is characterized by bimodality. The wide particle size range 0.2–2 μm is connected with the strong agglomeration of nanograins in the process of consolidation.

In Fig. 6, the microstructure of the sintered 78 vol.% Si_3N_4–22 vol.% ZrN specimen is shown. The structure of this composite is characterized by a bimodal grain size distribution. Zirconium nitride grains (light) have a relatively narrow size range of the order of 100–300 nm. At the same time, the Si_3N_4 phase (dark), whose content is about 80 vol.%, is characterized by a bimodal grain size distribution. Grains with a size of 100–300 nm and needle-like grains with a length up to several microns are present.

The mechanical characteristics of these materials are the following: the hardness is 22.5 ± 1.8 GPa, and the fracture toughness is 6.2 MPa. The high mechanical

Fig. 6 Microstructure of a
sintered 78 vol.% Si_3N_4–
22 vol.% ZrN
specimen
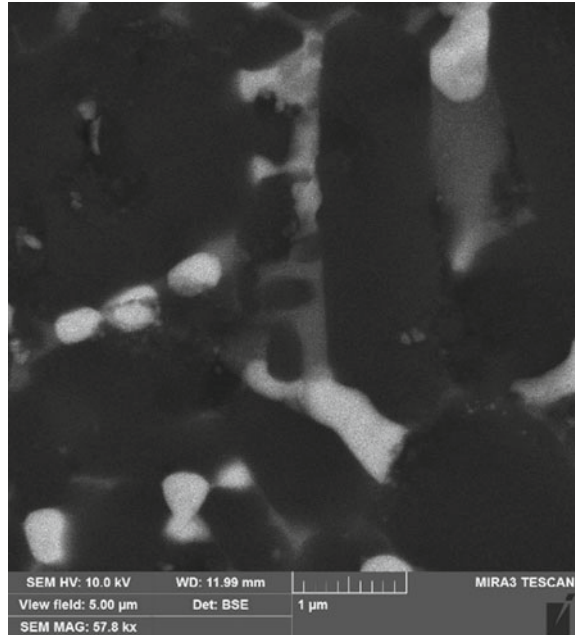
properties of the obtained material can be explained by the structural features of the
composite. The high hardness is achieved due to the decrease in the grain size down
to the nanolevel, and the presence of needle-like Si_3N_4 grains enhances the fracture
toughness of the composite.

5   Conclusions

The two-stage synthesis process of composite nanopowders in the Si_3N_4–ZrN system
is proposed. It has been established that the vacuum treatment process of the $Si_3N_4 +$
Zr reaction mixtures makes it possible to obtain a precursor containing all necessary
initial components of the nitride ceramics in the first stage of synthesis at a temper-
ature of 1000 °C. The performance of synthesis in a single cycle that combines the
processes of vacuum treatment (1000 °C) and nitriding (1200 °C) leads to obtaining
disperse powders of Si_3N_4–ZrN composite materials in the wide concentration range
11–33 vol.% ZrN. The obtained powder mixtures are characterized by the presence
of agglomerates up to several microns and nanosized particles.

The consolidation of the synthesized powders of the Si_3N_4–ZrN system has been
performed by spark plasma sintering at a temperature of 1750 °C under a pressure of
60 MPa. The composition with 33 vol.% ZrN has shown the best sinterability, which
is connected with the formation of a continuous conductive 3D network of ZrN
particles. Compact specimens made of the 67 vol.% Si_3N_4–33 vol.% ZrN composite

is characterized by a relative density above 97% and a bimodal structure, where grains with a size of ~200 nm and needle-like silicon nitride grains with a size up to several microns are present. The mechanical properties of this material are as follows: the hardness is 22.5 ± 1.8 GPa, and fracture toughness is 6.2 MPa.

References

1. Harrison RW, Lee WE (2016) Processing and properties of ZrC, ZrN and ZrCN ceramics: a review. Adv Appl Ceram 115:294–307
2. Krushinskaya LA, Makarenko GN, Oleynik GS, Uvarova IV, Fedorus VB (2007) Preparation of highly disperse composite powders of the Si$_3$N$_4$–TiN system. II. Structural-phase transformations during nitriding of titanium silicide powder. Nanostrukturnoe Materialovedenie (Nanostruct Mater Sci) 1:84–90 (in Russian)
3. Ade M, Haußelt J (2003) Electroconductive ceramic composites with low–to–zero shrinkage during sintering. J Eur Ceram Soc 23:1979–1986
4. Kurnetsov NT (1999) Precursors for carbide, nitride and boride synthesis. In: Gogotsi YG, Andrievski RA (eds) Materials science of carbides, nitrides and borides. NATO science series. Kluwer Academic Publishers, Dordrecht (Netherlands), pp 223–247
5. Kharlamov AI, Bondarenko ME, Rafal AN (1990) Kinetics of the interaction of transition metals with silicon nitride. In Collection of scientific works: silicides and their application in engineering. Institute for Problems of Materials Science of the Academy of Sciences of the Ukrainian SSR, Kiev (Ukrainian SSR), pp 35–40 (in Russian)
6. Polishchuk VS (2003) Intensification of the manufacturing processes of carbides, nitrides, and composite materials based on them. Veber, Sevastopol (Ukraine) (Polishchuk 2003) 7 (in Russian)
7. Zivkovic Lj, Nikolic Z, Boskovic S, Miljkovic M (2004) Microstructural characterization and computer simulation of conductivity in Si$_3$N$_4$–TiN composites. J Alloy Compd 373:231–236
8. Zivkovic LjM, Nikolic ZS, Boskovic SM (2002) Electrical properties and percolation concentration in Si$_3$N$_4$–TiN based composites. Key Eng Mater 206–213:1489–1492
9. Lux F (1993) Models proposed to explain the electrical conductivity of mixtures made of conductive and insulating materials. J Mater Sci 28:285–301
10. Zgalat-Lozynskyy OB, Herrmann M, Ragulya AV (2011) Spark plasma sintering of TiCN nanopowders in non-linear heating and loading regimes. J Eur Ceram Soc 31:809–813
11. Zgalat-Lozynskyy OB, Ragulya AV, Herrmann M, Andrzejczuk M, Polotai A (2012) Structure and mechanical properties of spark plasma sintered TiN-based nanocomposites. Arch Metall Mater 57:853–858
12. Zgalat-Lozinskii OB (2014) Nanocomposites based on refractory compounds, consolidated by rate-controlled and spark-plasma sintering. Powder Metall Met Ceram 53:19–30